Supporting Information for the manuscript entitled:

Effects of the oncogenic $V_{664}E$ mutation on membrane insertion, structure, and sequence-dependent interactions of the Neu transmembrane domain in micelles and model membranes: An integrated biophysical and simulation study

Andrew J. Beevers [‡], *Anthony Nash* [§], *Martha Salazar-Cancino* [‡], *David J. Scott* [||], *Rebecca Notman* [†,‡], *Ann M. Dixon** [‡]

‡ Department of Chemistry, [§]MOAC Doctoral Training Centre, and [†]Centre for Scientific Computing, University of Warwick, Coventry, CV4 7AL, UK.

|| Department of Biosciences, University of Nottingham, Nottingham, UK.

*To whom correspondence should be addressed: Telephone: +44 2476 150037; FAX: +44 2476 524112; email: ann.dixon@warwick.ac.uk

EXPERIMENTAL PROCEDURES

Molecular Dynamic Simulation

CHI Searches for initial dimer model building

To generate a starting structure for the dimer where the $I_{659}XXXV_{663}$ motif forms the primary binding interface, the Neu sequence was subjected to a global conformational search in vacuum using the CHI algorithm *(1)*. The distance between helices was set to 1.15 nm. Note that an inter-helical separation distance of ~1.1 nm is in agreement with the optimum distance found by previous conformational searches of Neu *(2)*. Right and left-handed crossing angles, as defined by the angle between the principle axis of each helix, were set to -25º and 25º

respectively. The helices were then rotated from 0º to 360º in increments of 10º. Each rotational step comprised four trial MD simulations of 5000 time-steps; for each trial the atomic velocities were assigned at random from a Maxwell-Boltzmann distribution. From the search results, topologies were collected using the CHI cluster calculation tool. The cut-off for the root mean squared difference between candidate structures was 0.1 nm. Up to eight structures within this cut-off constitute a complete cluster. The atomic positions of each member of the cluster are then averaged to yield a set of possible starting configurations for further MD simulation. A starting configuration was identified from these sets of clusters (Fig. S3).

Simulation Parameters

Force-field parameters for DPPC lipids were taken from the united atom force-field of Berger et al. *(3)*. Water was modeled using the simple point charge (SPC) model *(4)*. For the peptides the GROMOS96 53a6 set of parameters *(5)* were used. The ends of the peptides were terminated with neutral –NH2 and –COOH groups as charged groups would not normally exist at these positions in the native protein. The Arg and Lys residues within the helices were modeled in the protonated state. We chose to model the native peptide sequence with a Pro residue at position 655. Simulations were performed using the GROMACS simulation package, version 4.5.1. *(6-7)*. The Lennard-Jones interactions were cut off at 1.4 nm. For the electrostatic interaction, we used the particle-mesh Ewald method with a real-space cut off distance of 1.4 nm *(8-9)*. Simulations were performed in the NPT ensemble with semi-isotropic pressure coupling, where the simulation box in the direction of the bilayer normal (z-axis) and the cross-sectional area of the box in the x-y plane could vary independently. The temperature was maintained at 310 K using a Nose-Hoover thermostat *(10-11)*with a coupling time constant of 0.4 ps. The pressure was set at 1 bar and controlled by a Parrinello-Rahman barostat *(12-13)* with a coupling

time constant of 2 ps. The time step used in the simulations was 2 fs. All bonds in the system were constrained using the LINCS algorithm *(6)*.

Neu Protein-Bilayer Equilibration in Molecular Dynamics Simulation

The equilibration steps were as follows: (i) up to 10000 steps of steepest descents energy minimization to remove any initial atomic overlaps; (ii) 4 ns of simulation in the NVT ensemble with position restraints of 1000 kJ/mol on all the heavy atoms in the protein; (iii) three additional 6 ns simulations in the NPT ensemble with position restraints of 1000, 100 and 10 kJ/mol respectively on all the heavy atoms in the protein.

Supporting Figure S1. Circular dichroism spectra of the Neu and Neu* TM domain peptides containing the native Pro_{655} reconstituted in DMPC vesicles (fine solid line and fine dashed line, respectively) and Neu and Neu* TM domain peptides containing a Trp residue at position 655 reconstituted in POPC vesicles (bold solid line and bold dashed line, respectively). Apart from spectral differences at wavelengths below 200 nm that can be attributed to increased light scattering of POPC vesicles vs. DMPC vesicles, all four spectra show the characteristic α-helical signature (negative maxima at 208 and 222 nm) and all are very similar in magnitude, indicating similar helical content.

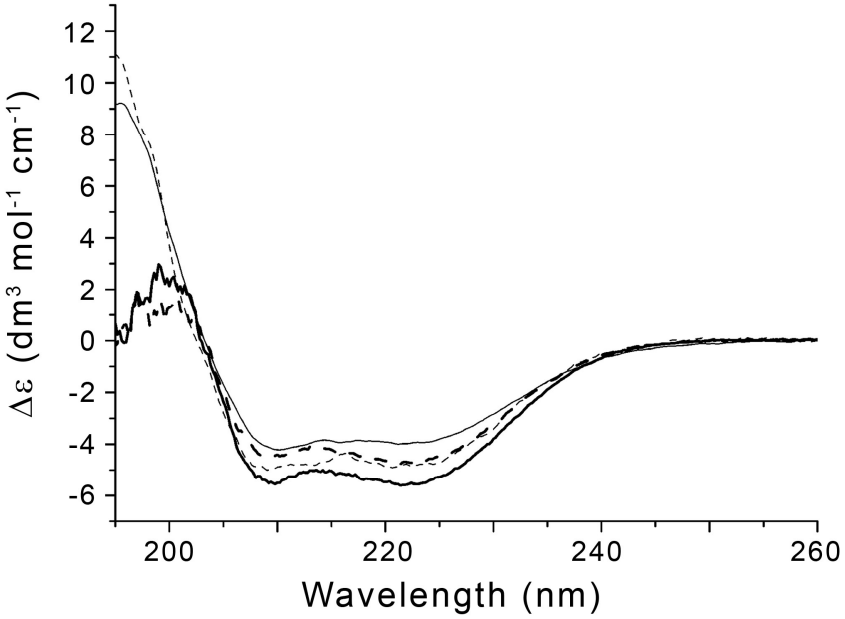

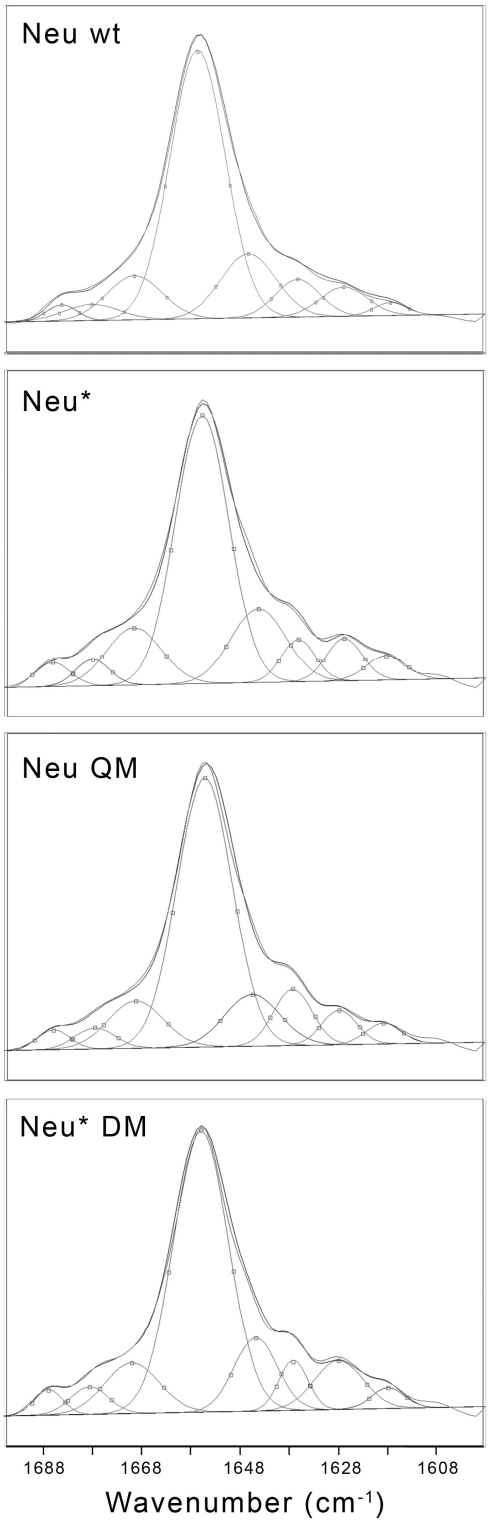

Supporting Figure S2. Transmission FTIR spectra of all four TM peptides studied after Fourier self-deconvolution *(14)* was carried out on the amide I region of the spectrum (1700-1600 cm^{-1}) using an enhancement factor of 2.0 and a bandwidth at half-height of 13 cm^{-1}. Fine lines show the Gaussian curves that produced the best fit to the data (fit carried out using GRAMS/AI software, Thermo Scientific). The curve of best-fit is shown as an overlay with the spectrum.

Supporting Figure S3. Initial configuration of the Neu complex generated from a global conformational search using CHI *(15)*. The peptide backbone is shown in grey ribbons and the $I_{659}XXXV_{663}$ motif is shown in space filling format.

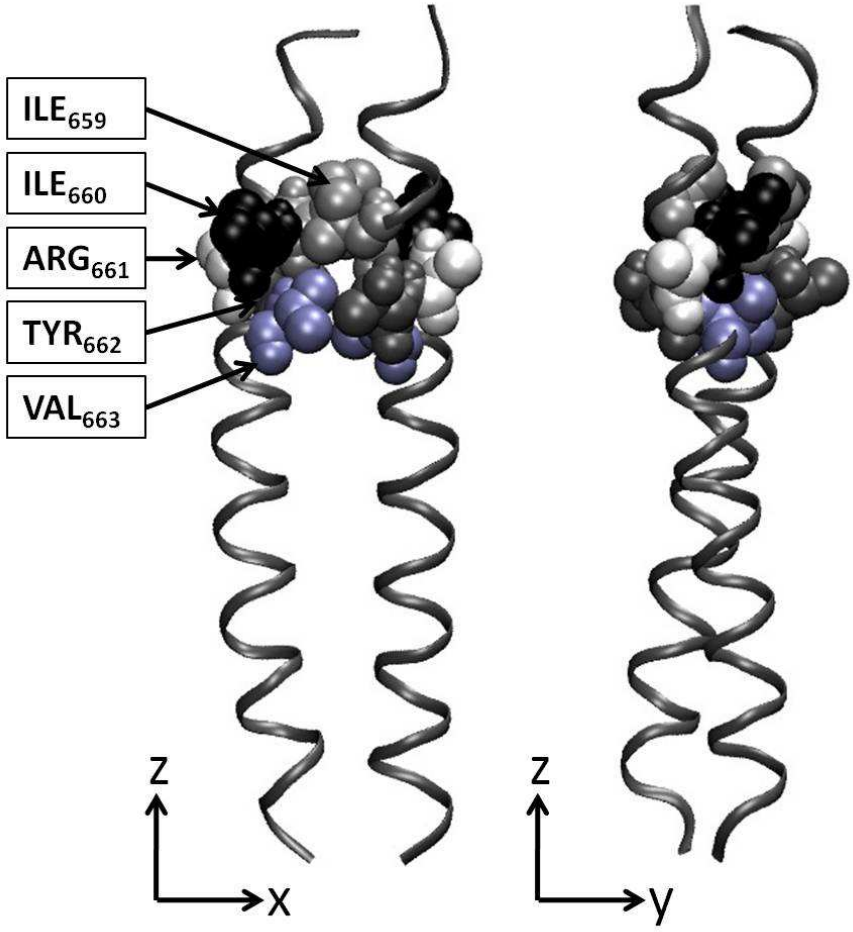

Supporting Figure S4. Distance of the centre of mass of the dimer to the centre of the bilayer as a function of time.

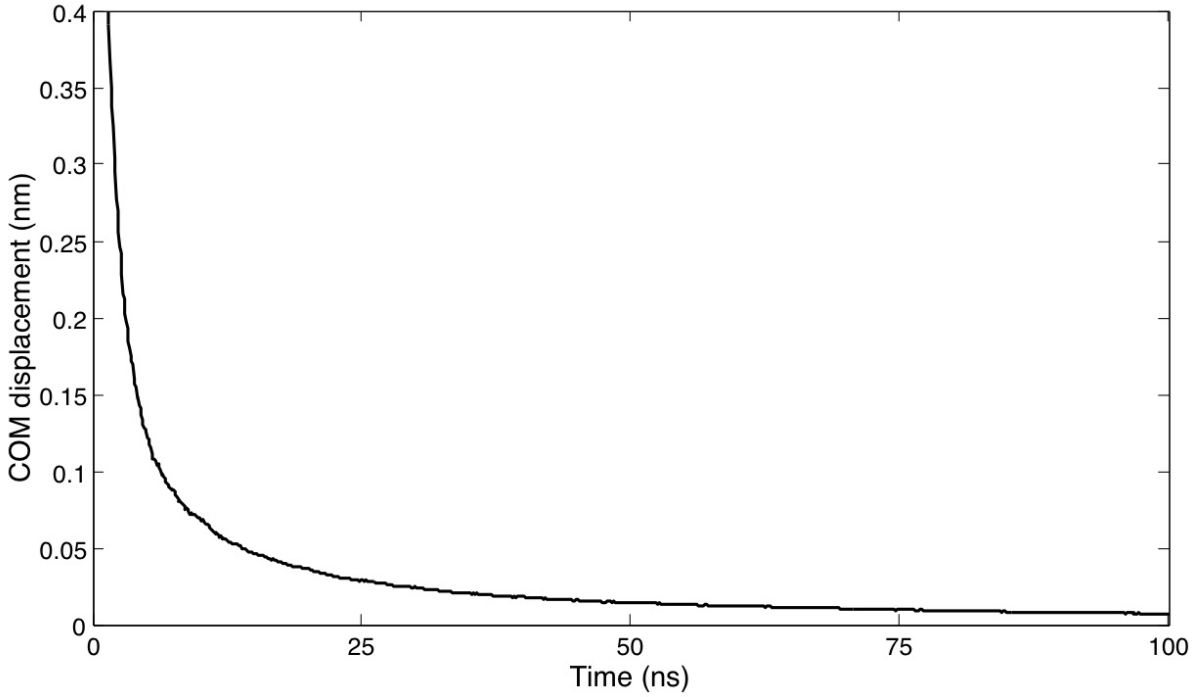

Supporting Figure S5. Percentage helicity of the dimer as a function of time.

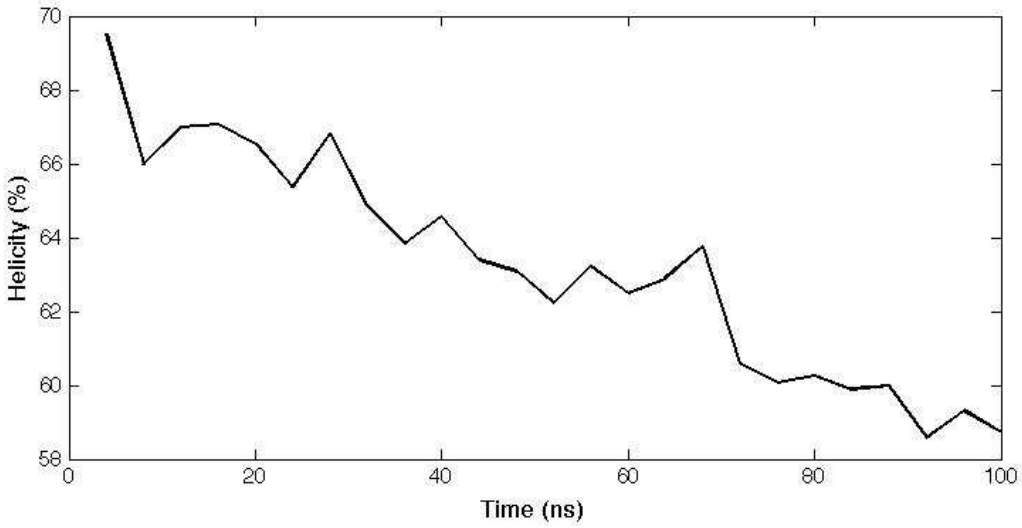

Supporting Figure S6. Percentage helicity per residue averaged over 0-20, 20-40, 40-60, 60-80 and 80-100 ns, for each of the helical peptides in the bilayer.

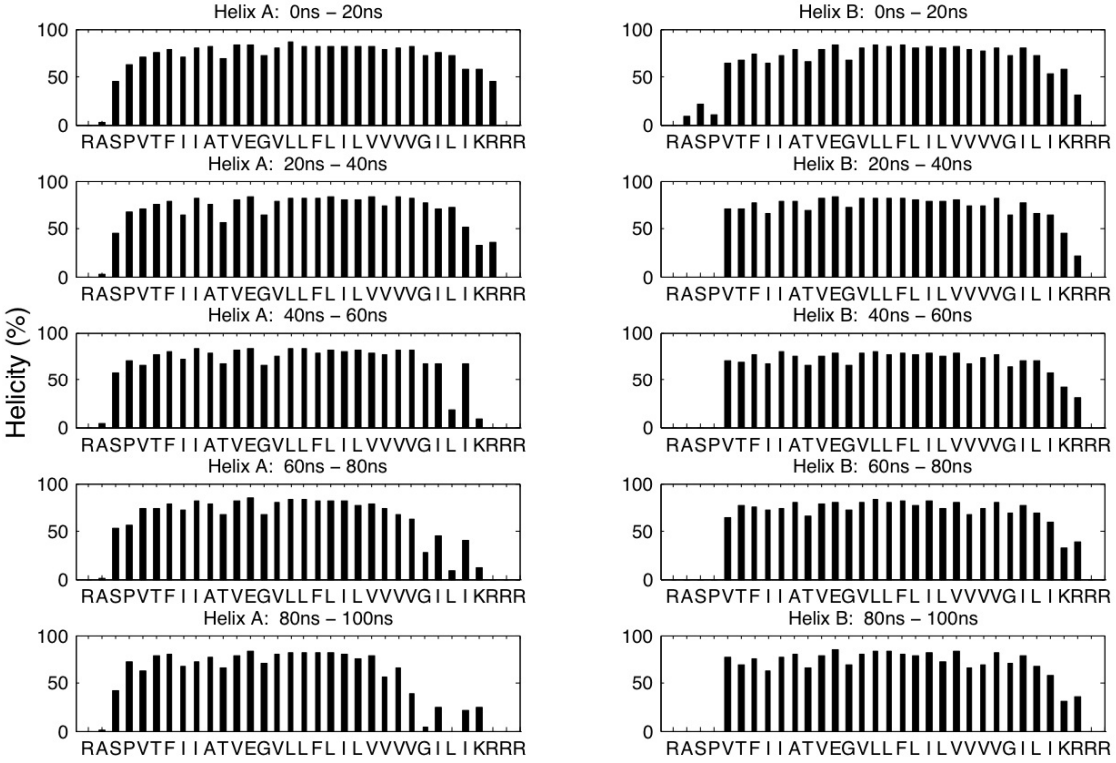

Supporting Figure S7. Distance between the two helices as a function of time computed from their crossing angle.

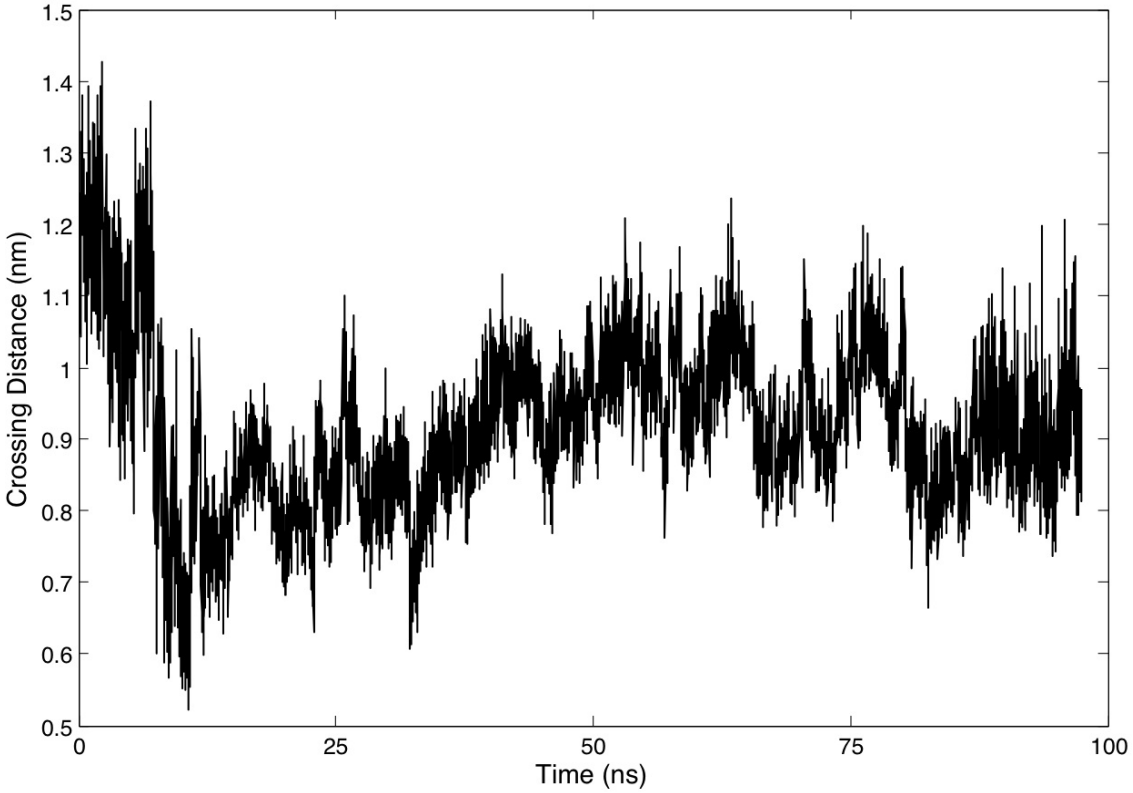

Supporting Figure S8. Inter-helical residue distance maps (in units of Angstroms) for the Neu dimer, averaged over the last 15 ns of the trajectory.

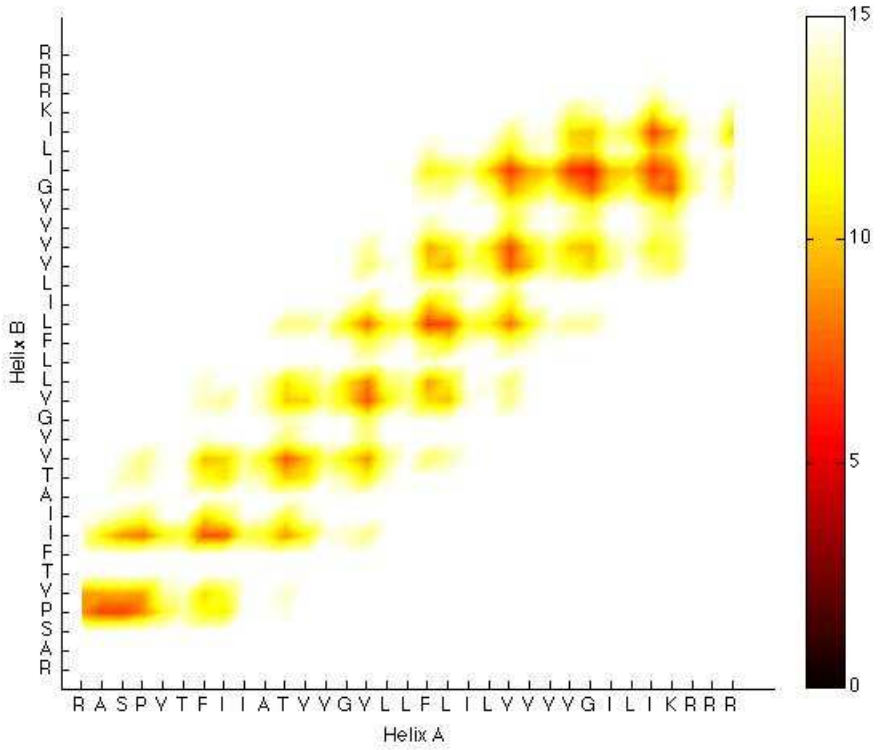

Supporting Table S1. Centers of the amide I and amide II bands in FTIR spectra of all four TM peptides in POPC bilayers, along with the full integrals of those bands before and after exposure to deuterium oxide in HDX experiments.

	Neu	**Neu***	**Neu_{QM}**	**Neu^*_{DM}**
frequency (cm^{-1}):				
amide I (center)	1656	1655	1655	1655
amide II (center)	1545	1544	1545	1545
Initial:				
amide I integral	7.13	12.03	6.03	6.92
amide II integral	2.26	3.64	1.62	2.02
1 hr. D_2O				
amide I integral	6.02	9.17	5.27	5.87
amide II integral	1.95	2.86	1.52	1.67
22 hr. D_2O				
amide I integral	6.27	9.69	5.43	5.91
amide II integral	1.93	2.95	1.41	1.44

REFERENCES

1. Adams, P.D., Arkin, I. T., Engelman, D. M., and Brunger, A. T. (1995) Computational searching and mutagenesis suggest a structure for the pentameric transmembrane domain of phospholamban, *Nat. Struct. Biol. 2*, 154-162.

2. Sajot, N. and Genest, M. (2000) Structure prediction of the dimeric neu/ErbB-2 transmembrane domain from multi-nanosecond molecular dynamics simulations, *Eur. Biophys. J. Biophys. Lett. 28*, 648-662.

3. Berger, O., Edholm, O. and Jahnig, F. (1997) Molecular dynamics simulations of a fluid bilayer of dipalmitoylphosphatidylcholine at full hydration, constant pressure, and constant temperature, *Biophys. J. 72*, 2002-2013.

4. Berendsen, H.J.C., Postma, J. P. M., van Gunsteren, W. F., and Hermans, J. (1981) Intermolecular forces (Pullman, B., Ed.) pp 331–342, Reidel Publishing Company, Dordrecht.

5. Oostenbrink, C., Villa, A., Mark, A.E., and Van Gunsteren, W.F. (2004) A biomolecular force field based on the free enthalpy of hydration and solvation: The gromos force-field parameter sets 53a5 and 53a6, *J. Comput. Chem. 25*, 1656-1676.

6. Hess, B., Kutzner, C., van der Spoel, D., and Lindahl, E. (2008) Gromacs 4: Algorithms for highly efficient, load-balanced, and scalable molecular simulation, *J. Chem. Theory Comput. 4*, 435-447.

7. Lindahl, E., Hess, B., and van der Spoel, D. (2001) Gromacs 3.0: A package for molecular simulation and trajectory analysis, *J. Mol. Model. 7*, 306-317.

8. Darden, T.A., York, D., and Pedersen, L. (1993) Particle-mesh ewald: An n.Log(n) method for ewald sums in large systems, *J. Chem. Phys. 98*, 10089-10092.

9. Essmann, U., Perera, L., Berkowitz, M.L., Darden, T., Lee, H., and Pedersen, L.G. (1995) A smooth particle mesh ewald method, *J. Chem. Phys. 103*, 8577-8593.

10. Hoover, W.G. (1985) Canonical dynamics: Equilibrium phase-space distributions, *Phys. Rev. A 31*, 1695-1697.

11. Nose, S.A. (1984) Molecular-dynamics method for simulations in the canonical ensemble, *Mol. Phys. 52*, 255-268.

12. Nose, S. and Klein, M.L. (1983) Constant pressure molecular dynamics for molecular systems, *Mol. Phys. 50*, 1055-1076.

13. Parrinello, M. and Rahman, A. (1981) Polymorphic transitions in single crystals: A new molecular dynamics method, *J. Appl. Phys. 52*, 7182-7190.

14. Kauppinen, J.K., Moffatt, D.J., Mantsch, H.H., and Cameron, D.G. (1981) Fourier self-deconvolution: A method for resolving intrinsically overlapped bands, *Appl. Spectr. 35*, 271-276.

15. Adams, P.D., Arkin, I. T., Engelman, D. M., and Brunger, A. T. (1995) Computational searching and mutagenesis suggest a structure for the pentameric transmembrane domain of phospholamban, *Nat. Struct. Biol. 2*, 154-162.